Journal of Molecular Catalysis A: Chemical 325 (2010) 48–54

Contents lists available at ScienceDirect

Journal of Molecular Catalysis A: Chemical

journal homepage: www.elsevier.com/locate/molcata

Photocatalytic degradation of polycyclic aromatic hydrocarbons in GaN:ZnO solid solution-assisted process: Direct hole oxidation mechanism

Jiahui Kou[a,b,c], Zhaosheng Li[a,c], Yong Guo[a,b,c], Jun Gao[a,c], Ming Yang[a,b,c], Zhigang Zou[a,b,c,*]

[a] Eco-materials and Renewable Energy Research Center (ERERC), Nanjing University, Nanjing 210093, PR China
[b] Department of Physics, Nanjing University, Nanjing 210093, PR China
[c] National Laboratory of Solid State Microstructures, Nanjing University, Nanjing 210093, PR China

ARTICLE INFO

Article history:
Received 22 December 2009
Received in revised form 23 March 2010
Accepted 23 March 2010
Available online 30 March 2010

Keywords:
Photodegradation
Polycyclic aromatic hydrocarbons
Solid solution
GaN
ZnO

ABSTRACT

The photooxidation of four polycyclic aromatic hydrocarbons (PAHs), namely phenanthrene (PHE), anthracene (ANT), acenaphthene (ACE), and benz[a]anthracene (BaA), were investigated. The solid solution GaN:ZnO before and after Pt modification were employed as photocatalysts. The intermediates from photodegradation were analyzed by gas chromatography–mass spectrometer. Active species in the present photocatalytic systems were monitored by the electron paramagnetic resonance spin-trap technique and hydrogen peroxide test strip. The effects of radicals and hole scavengers on the photocatalytic degradation of PAHs were also evaluated. The experimental results show that GaN:ZnO exhibits excellent activity for the photodegradation of PAHs, and the activity can be obviously improved by loading Pt. The reactivity of PAHs decreases in the order of PHE > BaA > ANT > ACE. On the catalyst of Pt–GaN:ZnO, PHE, BaA, ANT, and ACE can be degraded completely after 1, 3, 6, and 8 h visible light irradiation respectively. The mechanism examination evidences that the degradation of PAHs is induced by the formation of holes and active H species in the present photocatalytic system. The holes interact with PAHs to produce $PAHs^{+\bullet}$, which are active enough to react with O_2 and active H species. The theoretical calculation results display that the active positions of PAHs without sp^3 orbital hybridization can be predicted by the frontier electron density (f_r).

1. Introduction

The removal of polycyclic aromatic hydrocarbons (PAHs) has attracted considerable attention owing to their widespread environmental distribution, toxicity, and carcinogenicity [1,2]. The high stability and lipid solubility of PAHs lead to their accumulation in organism. Human beings are on the top of food chain, and therefore are the most greatly damaged. The US Environmental Protection Agency (EPA) has included 16 PAHs in the list of priority pollutants [3]. Many attempts have been made to remove these PAHs in the last decades. Microbial degradation is considered as a primary method for the elimination of PAHs in the environment [4]. However, the efficiency of bioremediation depends on the environmental conditions and is in general low. Up to now, the development of an effective method for PAHs degradation remains a challenge.

Due to the utilization of clean solar energy and no use for any additional chemicals, heterogeneous photocatalytic processes have attracted much interest. The semiconductor catalysts used for photocatalytic degradation have been studied extensively for the removal of organic pollutants in wastewater [2,5]. However, most current photocatalysts are metal oxides and usually work in the ultraviolet region because of their inherent large band gaps [6]. Aiming at enhancing the light absorption efficiency, many efforts have been dedicated to decrease the band gap of photocatalysts. Recently, materials derived from the solid solution GaN:ZnO have become a focus of interest [7–9]. The solid solution GaN:ZnO is a new type of oxynitride with a wurtzite-type structure, and is classified as a material containing d_{10} typical metal cations. The presence of Zn 3d and N 2p electrons in the upper valence band provides p–d repulsion for the valence band maximum, which results in the narrowing of band gap [10,11]. This solid solution represents a successful example of overall water splitting through photocatalytic reactions with a band gap in visible region (<3 eV) [7]. The ability for water splitting into O_2 indicates the strongly oxidative potential of photoinduced hole. The photocatalytic splitting of water over GaN:ZnO has been widely studied [7–9,12]. To the best of our knowledge, however, the literature concerning the degradation of contamination over GaN:ZnO are very scare, if any. It is thus desirable to investigate the photooxidation of PAHs using GaN:ZnO as photocatalyst, not only for the degradation of PAHs but also for

* Corresponding author at: Department of Physics, Nanjing University, 22 Hankou Road, Nanjing 210093, PR China. Tel.: +86 25 83686630; fax: +86 25 83686632.
E-mail address: zgzou@nju.edu.cn (Z. Zou).

1381-1169/$ – see front matter © 2010 Elsevier B.V. All rights reserved.
doi:10.1016/j.molcata.2010.03.029

the determination of photocatalytic property and mechanism of GaN:ZnO.

In the present study, we employed the solid solution GaN:ZnO as photocatalyst. The effect of loading Pt cocatalyst was examined. Four typical PAHs, namely phenanthrene (PHE), anthracene (ANT), acenaphthene (ACE), and benz[a]anthracene (BaA) were used as reactants. The photocatalytic degradation behavior of these PAHs was well investigated. The degradation mechanism over GaN:ZnO was also examined.

2. Experimental

2.1. Materials preparation and characterization

The GaN:ZnO solid solution was prepared by heating a mixture of Ga_2O_3 and ZnO powders under flowing NH_3 (80 mL min^{-1}) at 850 °C for 15 h [7]. The molar ratio of Zn to Ga (Zn/Ga) in the starting material (ZnO and Ga_2O_3) was 0.5, 1, and 2, represented as Zn/Ga 0.5, Zn/Ga 1, and Zn/Ga 2, respectively. Pt (0.5 wt.%) was loaded on GaN:ZnO by the photocatalytic reduction of H_2PtCl_6 in methanol aqueous solution under full arc light irradiation for 8 h (300 W Xenon lamp). The crystal structures of the obtained samples were examined by X-ray diffractometer (XRD) (Utilma III Tokyo, Japan). The morphology and dispersion of deposited Pt particles were detected by transmission electron microscopy (TEM) (FEI, Tecnai 20, USA). The optical absorption spectra of GaN:ZnO samples were recorded by ultraviolet–visible spectrophotometer (UV–vis) (Shimadzu UV–2550, Japan). The surface atomic percentages of Zn, Ga, N, and O were estimated from the areas of the X-ray photoelectron spectra (XPS) (Thermo Fisher Scientific, USA) peaks.

2.2. Photocatalytic reactions

Photocatalytic reactions were carried out in a 100 mL quartz reaction cell. To prevent the thermal catalytic effect, the reaction cell was dipped into a water cooler trough. In a typical experiment, 3 mg of PAH was first dissolved in the solvent consisted of 30 mL of water and 30 mL of acetone. In the experiment of determining active species, the amount of KI and benzoquinone were both 2×10^{-4} mol. The solution of PAH was then added into the quartz cell containing a certain amount of photocatalyst. The suspension was magnetically stirred in the dark for 2 h before irradiation to ensure the establishment of an adsorption/desorption equilibrium of PAH on the photocatalyst surface. Subsequently, the quartz cell was immersed in an ice–water mixture, followed by irradiation with a 300 W Xenon lamp equipped with a cut-off filter ($\lambda > 420$ nm). After the reaction, the slurry of reaction mixture was taken out and centrifuged to remove the photocatalyst. The products were extracted with dichloromethane. The dichloromethane layer dried by anhydrous sodium sulfate was quantified by GC (Agilent 6890N, USA) and identified by GC–MS (Agilent 6890N/5973I, USA). The GC was equipped with a flame ionization detector and a split/splitless injector. The injection mode was split injection with the split ratio of 16.5:1. An HP-5 column was used for separation (30 m, 0.25 mm I.D., 0.25 μm film thickness). The quantification was based on the external standard and the use of calibration curve. The intermediates were identified by comparing the mass spectra with authentic ones in the NIST 02 library. Mass spectra were recorded at 1 scan s^{-1} under the electron impact of 70 eV and mass range of 30–350 amu.

The existence of hydrogen peroxide in the photocatalytic reaction solution was examined by hydrogen peroxide test strip. To determine the active oxygen species in the system, the DMPO–free-radicals were detected at room temperature by a Bruker electron paramagnetic resonance (EPR) 10/12 spectrometer. The EPR instrument was operated at the microwave frequency of 9.76 GHz, the microwave power of 0.02 W, and the modulation frequency of 100 kHz. The highest occupied molecular orbital (HOMO) and lowest unoccupied molecular orbital (LUMO) for each PAH position in water and acetone were calculated by Gaussian 03 with the B3LYP functional and 6-31g(d) basis sets. Then, the frontier electron density was calculated [13].

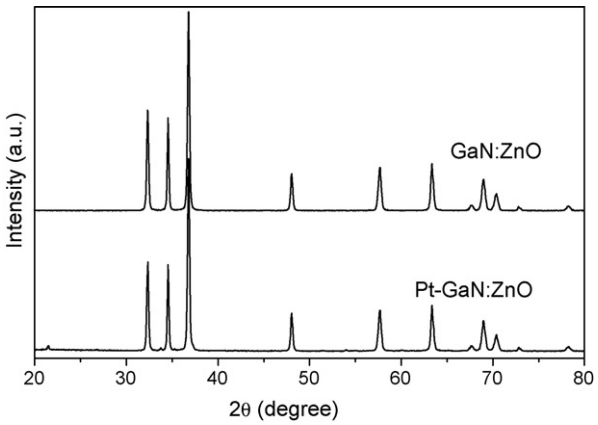

Fig. 1. XRD patterns of GaN:ZnO and Pt–GaN:ZnO.

3. Results and discussion

3.1. Photocatalyst characterization

Fig. 1 shows the XRD patterns of GaN:ZnO and Pt–GaN:ZnO samples. The sharp diffraction lines indicate that the solid solutions are well crystallized. The patterns of GaN:ZnO before and after Pt loading are quite similar, and all diffraction lines can be assigned to GaN:ZnO [7]. This imply that GaN:ZnO is stable under light irradiation, since Pt was loaded on GaN:ZnO by the photodeposition method. Due to its low amount, no Pt phase is detected in the XRD pattern of Pt–GaN:ZnO. However, spherical or hemispherical Pt particles with the diameter of 1–3 nm are observed in TEM image (Fig. 2), suggesting that Pt is successfully deposited

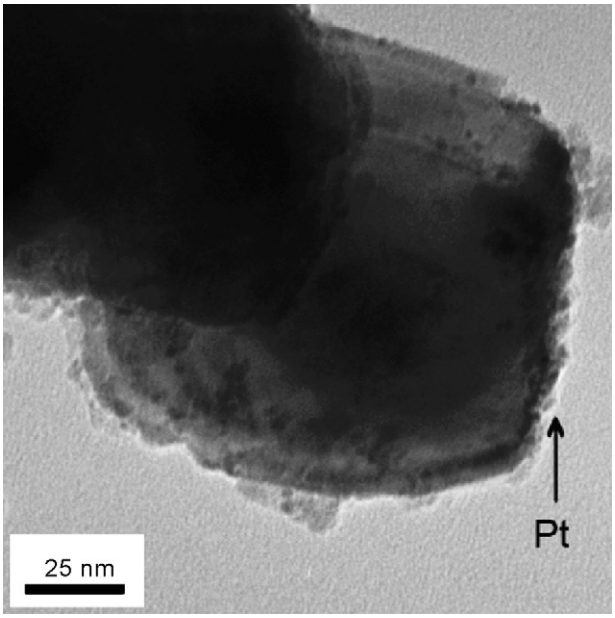

Fig. 2. TEM image of Pt–GaN:ZnO.

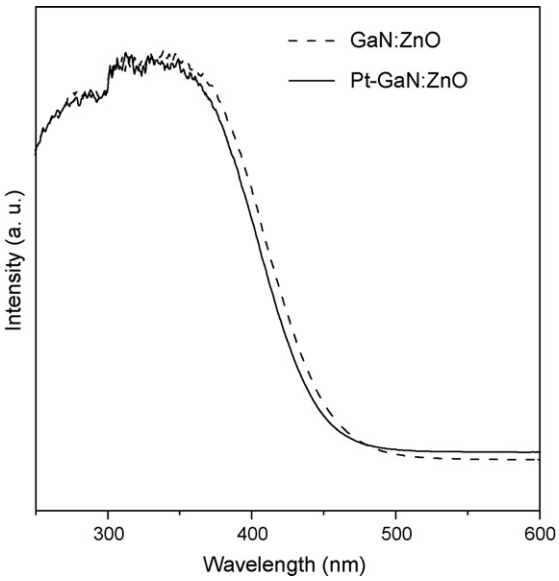

Fig. 3. UV–vis absorption spectra of GaN:ZnO and Pt–GaN:ZnO.

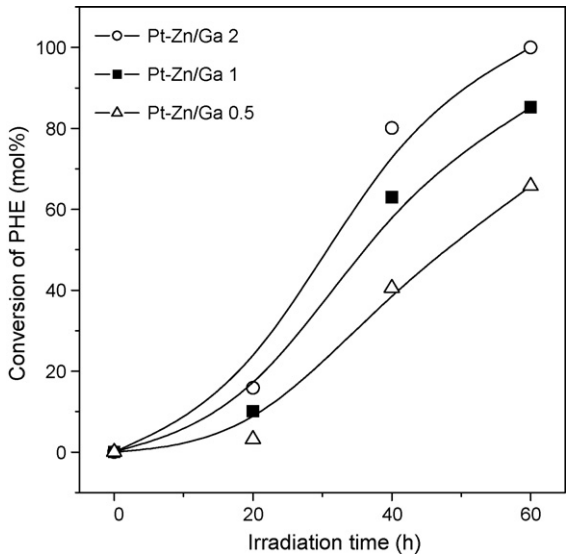

Fig. 4. Relationship between the conversion of PHE and the molar ratio of Zn to Ga (Zn/Ga) in the starting material.

onto the surface of GaN:ZnO. Fig. 3 displays the UV–vis absorption spectra of GaN:ZnO before and after Pt loading. No obvious difference in absorption edge is observed in two spectra. According to the absorption band-edge of about 470 nm, the band gap can be estimated to be 2.6 eV [14]. Table 1 shows the surface atomic compositions of Zn, Ga, N, and O, which were estimated from the peak areas of the XPS. With the increase of the starting Zn/Ga ratio, the Zn/Ga ratio in GaN:ZnO samples are enhanced as well as the O/N ratio.

3.2. Photodegradation of PAHs

The relationship between the conversion of PHE and the molar ratio of Zn/Ga is illustrated in Fig. 4. In the three samples of Pt loading Zn/Ga 0.5, Zn/Ga 1, and Zn/Ga 2, the Zn/Ga 2 has the highest activity. Hereinafter, the molar ratio of Zn/Ga in the starting material is 2. Fig. 5 displays the effect of irradiation time on the photodegradation of PHE over GaN:ZnO and Pt–GaN:ZnO. With the prolonging of irradiation time, the conversion of PHE increases over GaN:ZnO. About 15% of PHE is converted in 1 h. It is worth noting that the introduction of Pt promotes the activity of GaN:ZnO dramatically. PHE can be completely converted over Pt–GaN:ZnO in 1 h. In the initial stage, the reaction rate of PHE over Pt–GaN:ZnO is about 10 times higher than that over GaN:ZnO. Similar effect of Pt is also observed on the photodegradation of BaA, ANT, and ACE. The conversion of 100% can be obtained for BaA, ANT, and ACE over Pt–GaN:ZnO in 3, 6, and 8 h respectively. At the same reaction time, nevertheless, the conversion of BaA, ANT, and ACE over GaN:ZnO is only 71, 25, and 32% respectively. Because the absorption edge of GaN:ZnO before and after loading Pt is essentially the same (Fig. 3), the activity difference between two catalysts cannot be attributed to the distinction of their light absorption. The efficient electron trap ability of Pt that prevents the electron–hole recombination in

Table 1
Surface atomic composition in GaN:ZnO samples.

Sample	Elements (atom %)			
	Ga	Zn	O	N
Zn/Ga 2	30.2	2.2	27.9	39.8
Zn/Ga 1	32.2	1.8	20.3	45.7
Zn/Ga 0.5	34.5	1.7	15.6	48.2

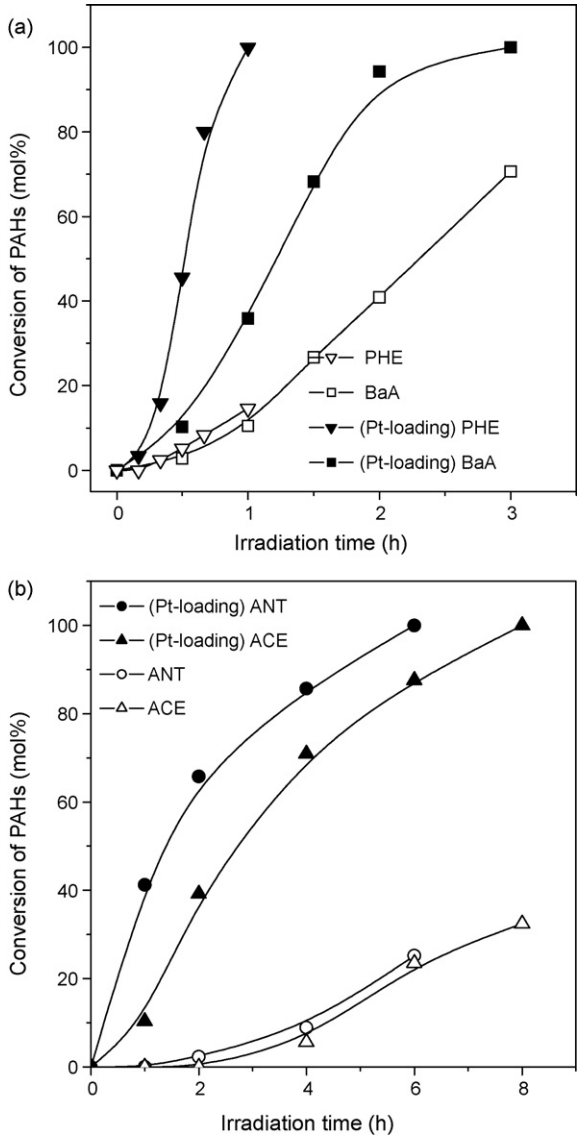

Fig. 5. Effect of irradiation time on the conversion of PAHs over GaN:ZnO or Pt–GaN:ZnO under visible light irradiation. (a) PHE and BaA and (b) ACE and ANT.

Table 2
Structure of PAHs under study and corresponding intermediates.

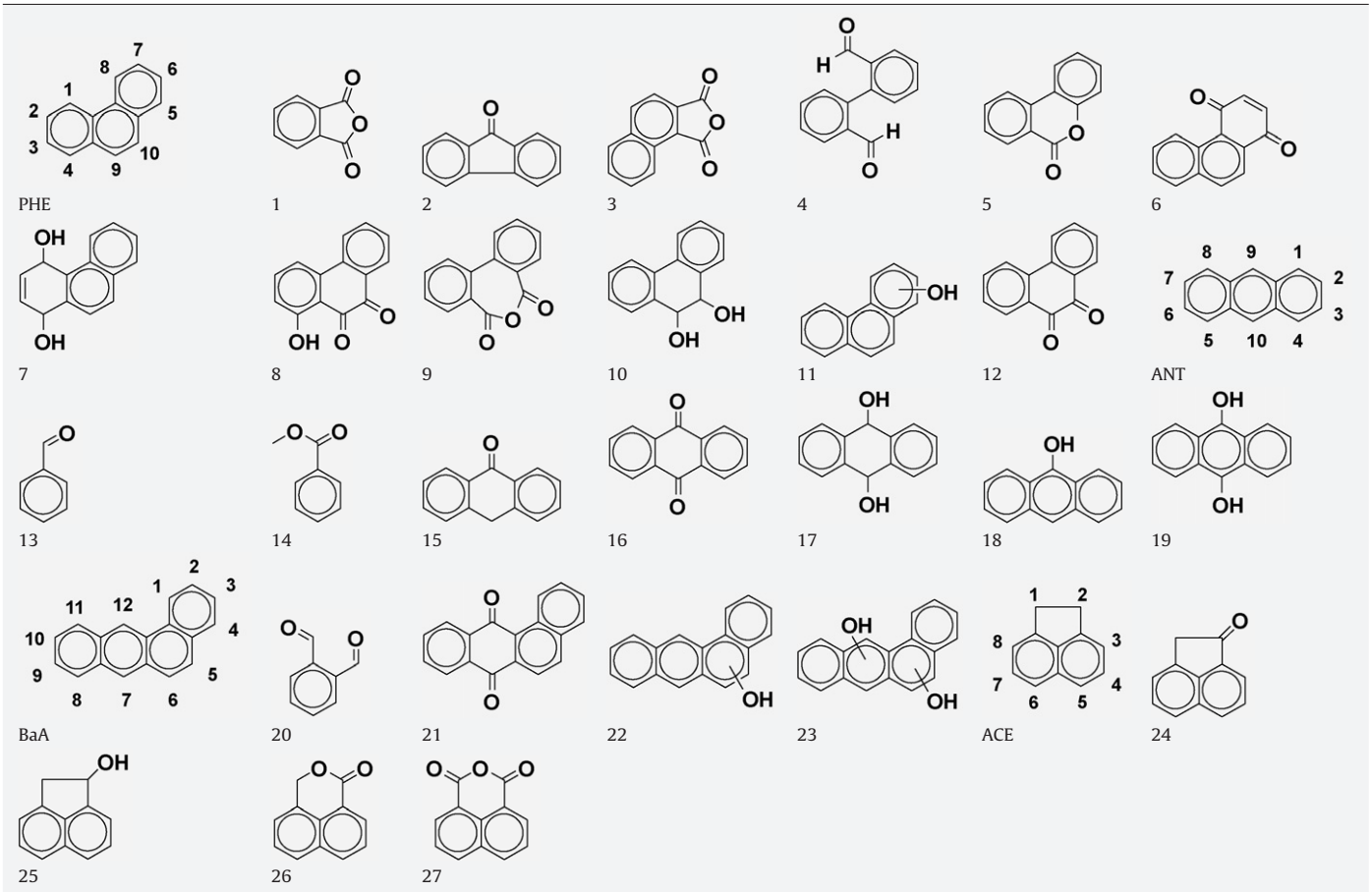

GaN:ZnO may be responsible for such difference [15]. It can also be seen from Fig. 5 that the reactivity of PAHs decreases in the order of PHE > BaA > ANT > ACE. However, several reports indicate that ANT is more active than PHE in some reactions, such as Fenton reaction [16] and $BiVO_4$ photocatalysis system [17]. It should be stated that $HO^{\bullet}$ radical is determined as the main active species in such reactions. In the present system, the photooxidation mechanism of PAHs is quite different as will be discussed later.

Table 2 summarizes the structure of PAHs and corresponding degradation products, which is one-to-one corresponding to peaks in Figs. 6 and 7, and Figs. S1–S4. Fig. 6 shows the total ion chromatogram and mass spectra of peaks ***7*** and ***10*** from PHE photooxidation. The mass spectra of other main peaks are displayed in Fig. S1. Although the conversion of PHE over GaN:ZnO is different from that over Pt–GaN:ZnO, the intermediates detected are quite similar. The main intermedia are compounds **4** and **12**, which come from the oxidation of 9 and 10 positions of PHE. Two isomers (namely peaks ***7*** and ***10***) with identical molecular ion of 212 were detected from the photodegradation of PHE. According to the standard spectra in library data, peak ***10*** can be assigned to 9,10-dihydro-9,10-dihydroxyphenanthrene. Correspondingly, peak ***7*** can be tentatively ascribed to 1,4-dihydro-1,4-dihydroxyphenanthrene by analyzing the fragmentation pattern of mass spectra. It is noticeable that compounds **7** and **10** are two hydrogenated–oxidation products. Hence, the oxidation of PHE in the present photocatalytic process accompanies with hydrogenation. Also, compound with the molecular ion of 212 (peak ***17***) is detected in the intermediates of ANT, as shown in Fig. 7. According to the fragmentation pattern of mass spectra, peak ***17*** can be assigned to 9,10-dihydro-9,10-dihydroxyanthracene. This gives further evidence that the hydrogenation of PAHs occurs in the process of photooxidation. To clarify the hydrogenation reaction, D_2O was used instead of H_2O in the photocatalytic system. Unfortunately, both PHE and ANT cannot be oxidized even after 6 h, possibly owing to the difference of chemical properties between H_2O and D_2O [18]. It is interesting to observe the yield of compounds **3** and **6** from PHE photodegradation over GaN:ZnO. These side-ring oxidation intermediates are absent on the catalysis of TaON [2]. Because the side-ring of PHE is more difficult to be oxidated than middle-ring, it can be inferred that the photoinduced oxidation ability of GaN:ZnO is stronger than that of TaON.

Fig. 7 and Fig. S2 show the total ion chromatogram and mass spectra of corresponding products from ANT photooxidation. Anthraquinone (compound **16**) is the predominant intermediate, and derives from the oxidation of 9 and 10 positions of ANT. In the initial stage, the reaction rate is very fast, and the conversion of ANT reaches 41% in 1 h over Pt–GaN:ZnO. However, the rate decreases in the succeeding reaction time. The intermediates from ANT photodegradation include anthrone (compound **15**), hydroxyl anthracene (compound **18**), dihydroxyl anthracene (compound **19**) and so on; these compounds are more active than ANT. As a result, competitive reaction between ANT and intermediates occurs, which leads to the decrease of reaction rate of ANT after 1 h.

The total ion chromatograms and corresponding mass spectra of products from the photodegradation of BaA and ACE are shown in Figs. S3 and S4, respectively. Benzanthraquinone (compound **21**) is the main oxidation product of BaA, indicating that 7 and 12 positions of BaA are the most active. The existence of hydroxylbenz[a]anthracenes (compound **22**, molecular ion: 244)

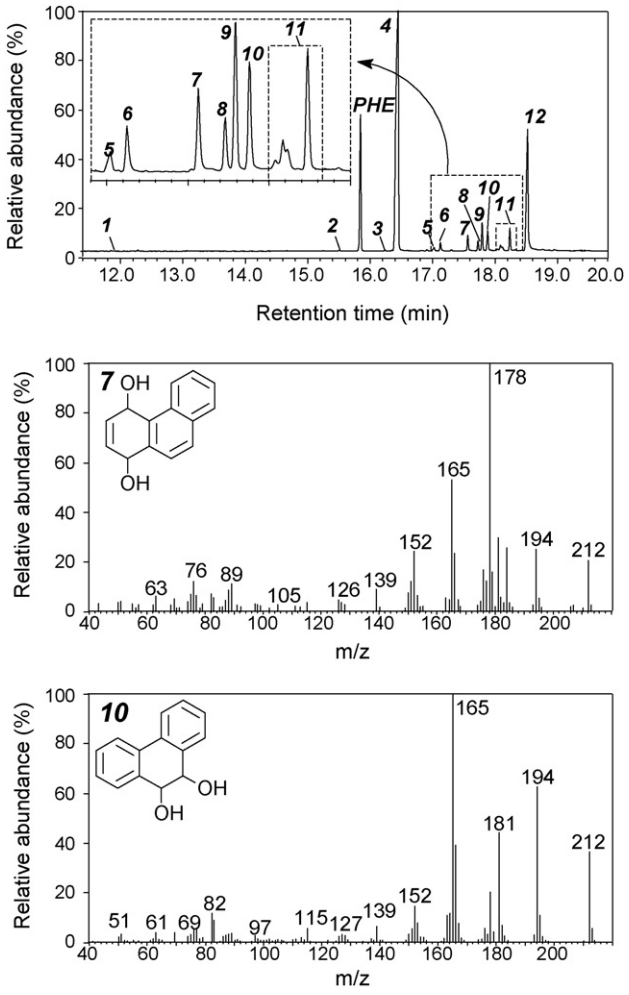

Fig. 6. Total ion chromatogram and the mass spectra of products 7 and 10 from PHE photodegradation over Pt–GaN:ZnO after 40 min visible light irradiation.

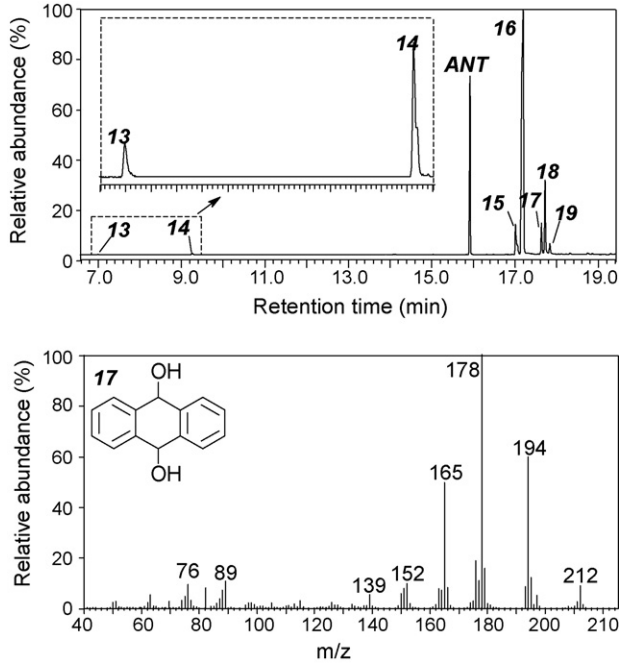

Fig. 7. Total ion chromatogram and the mass spectra of product 17 from ANT photodegradation over Pt–GaN:ZnO after 2 h visible light irradiation.

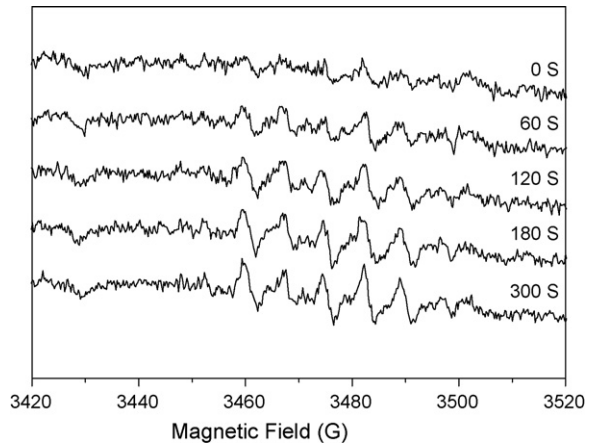

Fig. 8. EPR spectra of DMPO–$O_2^{-\bullet}$ adducts generated in the suspended liquid of GaN:ZnO under light irradiation.

can be confirmed, but an apparent difference in the retention time (Fig. S3) indicates that there are several isomers of hydroxylbenz[a]anthracene. The isomers should derive from the different position of the hydroxyl groups, although the positional determination of hydroxyl group is difficult from GC–MS analysis. Similarly, peak ***23*** (molecular ion: 260) are isomers of dihydroxylbenz[a]anthracene because of the different position of hydroxyl groups. The selectivity of hydroxylbenz[a]anthracenes and dihydroxylbenz[a]anthracenes is high in the initial stage. With the increase of reaction time, the selectivity decreases, since they are converted to deep oxidation products such as benzanthraquinone and small organic molecules. The oxidation of ACE initiates at 1 position and produces 1-hydroxylacenaphthene (compound **25**), which can be further oxidized to acenaphthenone (compound **24**). These two compounds are the main oxidation intermediates of ACE. With increasing reaction time, some deep oxidation products such as compounds **26** and **27** can be yielded.

3.3. Photocatalytic mechanism

In the absence of photocatalyst, the conversion of BaA is only 4% after 6 h irradiation, while PHE, ANT, and ACE were not converted at all. Moreover, the PAHs cannot be oxidized even after 6 h irradiation in the dark. These factors imply that the degradation of PAHs involve in the photocatalytic role of GaN:ZnO or Pt–GaN:ZnO in the present reaction system. To examine the effect of O_2 on the photodegradation of PAHs, the experiments excluded O_2 were carried out. The results show that no PAH is converted at all after 6 h irradiation. This indicates that O_2 also plays an important role in the photooxidation of PAHs. As mentioned above, PAHs cannot be oxidized after 6 h without light irradiation, which suggests that O_2 cannot oxidize PAHs directly. On the basis of these results, it is reasonable that other active species exist in the reaction system.

In semiconductor photocatalytic processes, photoinduced oxide radicals, hydrogen peroxide, and holes always play crucial roles in the degradation of organic substances [5]. The EPR spin-trap technique, which has been proved to be a useful method for the determination of oxide radicals [19,20], was first employed. No signal is detected in the dark. Under light irradiation, six characteristic peaks of DMPO–$O_2^{-\bullet}$ adducts [21–23] are observed in GaN:ZnO system, and the peak intensity increases with the prolonging of irradiation time (Fig. 8). The results imply the formation of $O_2^{-\bullet}$ radicals in GaN:ZnO system. Furthermore, no characteristic peak of DMPO–OH• adducts is found, implying that the active oxygen in the photocatalytic system of GaN:ZnO is different from conventional photocatalyst TiO_2 [23–25]. Interestingly, the signal

of DMPO–$O_2^{-\bullet}$ is not determined over Pt–GaN:ZnO, though the activity of Pt–GaN:ZnO is higher than GaN:ZnO. It is well known that multielectron reduction of molecular oxygen proceeds readily on the surface of platinum, which produces H_2O_2 or H_2O [26,27]. Therefore, it is expected that the multielectron reduction, which does not produce radical species of oxygen, takes place over the Pt–GaN:ZnO photocatalyst. To examine the role of $O_2^{-\bullet}$ anions in these photocatalytic systems, experiments in the presence of benzoquinone ($O_2^{-\bullet}$ anions radical scavengers) were carried out. Benzoquinone has the potential to trap superoxide anions by an electron transfer mechanism (Eq. 1) [28].

$$BQ + O_2^{-\bullet} \rightarrow BQ^{-\bullet} + O_2 \quad (1)$$

It is noticeable that the present of 2×10^{-4} mol benzoquinone has no effect on the photodegradation of PAHs in the system of either GaN:ZnO or Pt–GaN:ZnO. This implies that the $O_2^{-\bullet}$ anions are not the main active species in the present systems.

The existence of hydrogen peroxide in the photocatalytic reaction solution was examined by hydrogen peroxide test strip. The results show that no hydrogen peroxide exists in the system of GaN:ZnO or Pt–GaN:ZnO. The minimum detectability of this hydrogen peroxide test strip is 1 mg/L. Consequently, even if hydrogen peroxide exists in the system, its concentration should be less than 1 mg/L. Further experiment was also conducted in the system with the addition of 1 mg/L hydrogen peroxide. In such system, PHE cannot convert in the absence of photocatalyst. On the basis of these results, it is clear that hydrogen peroxide is not the active species in the present systems.

It has been demonstrated that neither oxide radicals nor hydrogen peroxide is the main active species in the GaN:ZnO and Pt–GaN:ZnO systems. The photoinduced holes should thus be responsible for the degradation of PAHs. Iodide is known as an effective hole scavenger [28–30]; iodine anions can react with holes to conduce their quench, as shown in Eqs. (2)–(4).

$$h^+ + I^- \rightarrow I^\bullet \quad (2)$$

$$I^\bullet + I^- \rightarrow I_2^{\bullet -} \quad (3)$$

$$h^+ + I_2^{\bullet -} \rightarrow I_2 \quad (4)$$

In the presence of iodine anions, PHE is not converted at all even after 6 h irradiation. As a result, holes are the main active species in the reaction system of both GaN:ZnO and Pt–GaN:ZnO.

In terms of abovementioned factors, the reaction pathways of PAHs can be proposed. Photoinduced holes and active H are initially produced, followed by the reaction of holes with PAHs to produce $PAHs^{+\bullet}$, as given in Eq. (5).

$$h^+ + PAHs \rightarrow PAHs^{+\bullet} \quad (5)$$

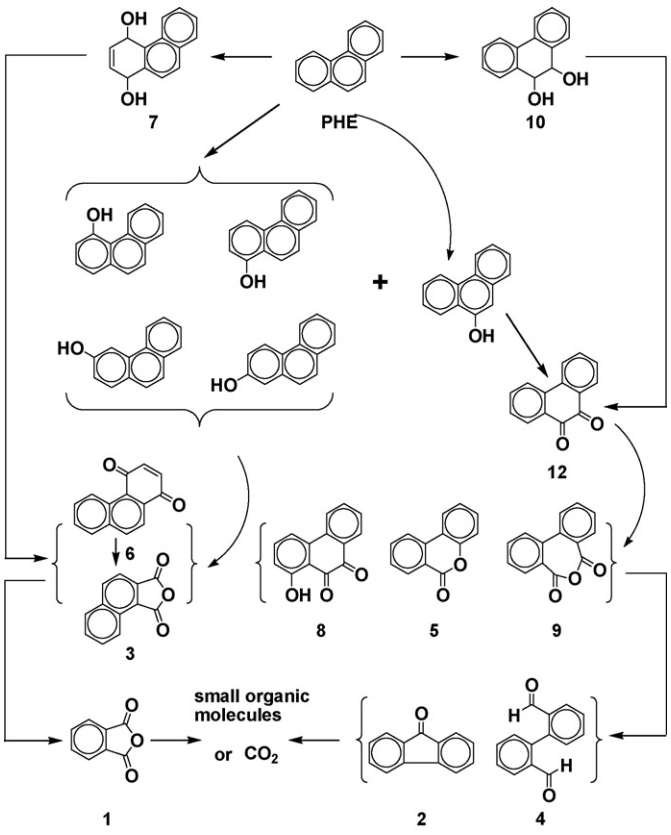

Scheme 1. Proposed pathways for PHE photodegradation in GaN:ZnO systems under visible light irradiation.

$PAHs^{+\bullet}$ are active enough to react with O_2 and active H species. The reaction pathways of PHE, ANT, BaA, and ACE are depicted in Scheme 1, and Schemes S1–S3, respectively. PAHs are firstly hydroxylated and hydrogenated to form hydroxyl compounds or hydrogenated hydroxyl intermediates. With the increase of reaction time, these intermediates are further oxidized to ketones or quinones. Finally, deep oxidation of the intermediates occurs and small molecules such as CO_2 are produced.

3.4. Theoretical calculation

It is well known that each atomic orbital can produce the frontier movement (C_{ri}). The Frontier electron density (f_r) can be calculated using the coefficient of each atomic orbital [31]. The positions where the highest density of two electrons $[2(C_{ri}^{HOMO})^2]$ occur when they are in the HOMO at ground state for an electrophilic reaction.

Table 3
f_r values of each position in PAHs.

Position	f_r (in acetone)				f_r (in water)			
	PHE	ANT	BaA	ACE	PHE	ANT	BaA	ACE
1	0.08773	0.16410	0.01365	0.00099	0.08740	0.16388	0.01377	0.00098
2	0.21787	0.10141	0.05842	0.00099	0.21783	0.10138	0.05842	0.00098
3	0.00090	0.10141	0.06310	0.11233	0.00090	0.10138	0.06317	0.11236
4	0.15848	0.16413	0.00640	0.16201	0.15848	0.16391	0.00643	0.16216
5	0.15853	0.16413	0.11409	0.30828	0.15852	0.16391	0.11392	0.30830
6	0.00090	0.10140	0.12854	0.30828	0.00090	0.10139	0.12850	0.30831
7	0.21789	0.10140	0.28571	0.16201	0.21784	0.10139	0.28600	0.16216
8	0.08778	0.16410	0.16948	0.11234	0.08744	0.16388	0.16913	0.11237
9	0.32115	0.28736	0.08967	–	0.32110	0.28787	0.08968	–
10	0.32116	0.28736	0.10394	–	0.32110	0.28787	0.10379	–
11	–	–	0.16259	–	–	–	0.16227	–
12	–	–	0.27333	–	–	–	0.27370	–

Because the active species holes are electrophiles, the reactions between PAHs and hole are electrophilic reactions. The calculation of f_r for a hole reaction can proceed via Eq. (6).

$$f_r = \Sigma_i(2(C_{ri}^{HOMO})^2) \quad (6)$$

In Eq. (6), r is the number of carbon atoms in i: 2s, $2p_x$, $2p_y$, and $2p_z$ orbitals. A higher f_r value implies a more active position. According to Gaussian 03 in conjunction with Eq. (6), the f_r values of different positions in PAHs were calculated and summarized in Table 3. For PHE, the f_r value in 9 and 10 positions are the highest in both acetone and water, indicating that the most active positions in PHE are 9 and 10 positions. Similarly, the most active positions are 9 and 10 positions in ANT, and 7 and 12 positions in BaA. The calculated results are in good agreement with the experimental ones, and the photocatalytic oxidation does take place at the most active positions initially. As shown in Table 3, the f_r values of 5 and 6 positions are the highest in ACE, which suggests that 5 and 6 positions should be the most active. Nevertheless, the experimental results display that 1 and 2 positions in ACE are the most readily to be oxidized. This can be explained as that the 1 and 2 positions of ACE have sp^3 orbital hybridization whereas the other positions of ACE have sp^2 orbital hybridization. Similar phenomenon was also reported in fluorene oxidation which has different molecule hybrid orbitals [31]. As a result, it is not accurate for molecule which has different molecule hybrid orbitals. On the basis of aforementioned results, it is conclusive that f_r value is an effective method to predict the active positions of PAHs without sp^3 orbital hybridization.

4. Conclusions

The solid solution GaN:ZnO exhibits excellent activity for the photodegradation of four typical PAHs (namely ANT, PHE, ACE, and BaA). Such activity can be greatly promoted by loading Pt. The reactivity of PAHs decreases in the order of PHE > BaA > ANT > ACE. On the catalysis of Pt–GaN:ZnO, PHE, BaA, ANT, and ACE can be degraded completely after 1, 3, 6, and 8 h visible light irradiation respectively. In the present system, the photooxidation of PAHs initializes by the formation of holes and active H. The succeeding interaction of holes and PAHs produces $PAHs^{+\bullet}$, which are active enough to react with O_2 and active H species, and finally are converted to small organic molecules or CO_2. The active positions of PAHs without sp^3 orbital hybridization can be predicted by f_r value. The present investigation may provide an alternative method for the photodegradation of PAHs as well as other organic contaminations.

Acknowledgements

Financial supports from the National Basic Research Program of China (973 Program, 2007CB613305), China–Japan Cooperation Project of Science and Technology (2009DFA61090), the Jiangsu Province Environmental Protection Bureau Scientific Research Project (No. 2008005), and the National Natural Science Foundation of China (No. 50732004) are gratefully acknowledged.

Appendix A. Supplementary data

Supplementary data associated with this article can be found, in the online version, at doi:10.1016/j.molcata.2010.03.029.

References

[1] Y.S. El-Alawi, B.J. McConkey, D.G. Dixon, B.M. Greenberg, Ecotoxicol. Environ. Saf. 51 (2002) 12–21.
[2] J. Kou, Z. Li, Y. Yuan, H. Zhang, Y. Wang, Z. Zou, Environ. Sci. Technol. 43 (2009) 2919–2924.
[3] M.A. Callahan, M.W. Slimak, N.W. Gabelc, I.P. May, C.F. Fowler, J.R. Freed, P. Jennings, R.L. Durfee, F.C. Whitmore, B. Maestri, W.R. Mabey, B.R. Holt, C. Gould, Water-related Environmental Fate of 129 Priority Pollutants, Washington, DC, U.S. Environmental Protection Agency, 1979, EPA-440/4-79-029.
[4] Y. Zeng, P.K. Angrew Hong, D.A. Wavrek, Water Res. 34 (2000) 1157–1172.
[5] M.R. Hoffmann, S.T. Martin, W. Choi, D.W. Bahnemann, Chem. Rev. 95 (1995) 69–96.
[6] A. Mills, S. Le hunte, J. Photochem. Photobiol. A 108 (1997) 1–35.
[7] K. Maeda, T. Takata, M. Hara, N. Saito, Y. Inoue, H. Kobayashi, K. Domen, J. Am. Chem. Soc. 127 (2005) 8286–8287.
[8] K. Maeda, K. Teramura, T. Takata, M. Hara, N. Saito, K. Toda, Y. Inoue, H. Kobayashi, K. Domen, J. Phys. Chem. B 109 (2005) 20504–20510.
[9] K. Maeda, K. Teramura, D. Lu, K. Takata, N. Saito, Y. Inoue, K. Domen, Nature 440 (2006) 295.
[10] W. Wei, Y. Dai, K. Yang, M. Guo, B. Huang, J. Phys. Chem. C 112 (2008) 15915–15919.
[11] K. Maeda, K. Domen, Chem. Mater. 22 (2010) 612–623.
[12] F.E. Osterloh, Chem. Mater. 20 (2008) 35–54.
[13] M.J. Frisch, et al., Gaussian 03, Revision E.01, Gaussian, Inc., Wallingford, CT, 2004.
[14] M.A. Butler, J. Appl. Phys. 48 (1977) 1914–1920.
[15] A.L. Linsebigler, G. Lu, J.T. Yates Jr., Chem. Rev. 95 (1995) 735–758.
[16] B.-D. Lee, J. Mater. Cycles Waste Manage. 2 (2000) 24–30.
[17] S. Kohtani, M. Tomohiro, K. Tokumura, R. Nakagaki, Appl. Catal. B 58 (2005) 265–272.
[18] S. Nakabayashi, A. Fujishima, K. Honda, Chem. Phys. Lett. 102 (1983) 464–465.
[19] J.R. Morton, Chem. Rev. 64 (1964) 453–471.
[20] H.V. Willigen, P.R. Levstein, M.H. Ebersole, Chem. Rev. 93 (1993) 173–197.
[21] W. Zhao, C. Chen, X. Li, J. Zhao, J. Phys. Chem. B 106 (2002) 5022–5028.
[22] Y. Che, W. Ma, Y. Ren, C. Chen, X. Zhang, J. Zhao, L. Zhang, J. Phys. Chem. B 109 (2005) 8270–8276.
[23] H. Fu, L. Zhang, S. Zhang, Y. Zhu, J. Phys. Chem. B 110 (2006) 3061–3065.
[24] P. Qu, J. Zhao, T. Shen, H. Hidaka, J. Mol. Catal. A 129 (1998) 257–268.
[25] C. Chen, X. Li, W. Ma, J. Zhao, J. Phys. Chem. B 106 (2002) 318–324.
[26] A. Fujishima, T.N. Tao, D.A. Tryk, J. Photochem. Photobiol. C 1 (2000) 1–21.
[27] U. Siemon, D. Bahnemann, J. Testa, D. Rodríguez, M. Litter, N. Bruno, J. Photochem. Photobiol. A 148 (2002) 247–255.
[28] R. Palominos, J. Freer, M.A. Mondaca, H.D. Mansilla, J. Photochem. Photobiol. A 193 (2008) 139–145.
[29] K. Ishibashi, A. Fujishima, T. Watanabe, K. Hashimoto, J. Photochem. Photobiol. A 134 (2000) 139–142.
[30] S. Yang, L. Lou, K. Wang, Y. Chen, Appl. Catal. A 301 (2006) 152–157.
[31] B.-D. Lee, M. Iso, M. Hosomi, Chemosphere 42 (2001) 431–435.